Design and Development of an Electromechanical Actuator Test Bench for Validation of Health Monitoring Models

# Design and development of an Electromechanical Actuator test bench for validation of health monitoring models

Pier Carlo Berri

*Dept. of Mechanical and Aerospace Engineering, Politecnico di Torino, Italy. E-mail: pier.berri@polito.it*

Matteo D.L. Dalla Vedova

*Dept. of Mechanical and Aerospace Engineering, Politecnico di Torino, Italy. E-mail: matteo.dallavedova@polito.it*

Paolo Maggiore

*Dept. of Mechanical and Aerospace Engineering, Politecnico di Torino, Italy. E-mail: paolo.maggiore@polito.it*

Electromechanical Actuators (EMAs) for aircraft flight controls are progressively replacing hydraulic systems in safety-critical applications. Hence, simple and accurate EMA numerical models are required for the real-time health monitoring of such equipment, as well as more detailed and computationally intensive simulations for design and training of machine learning surrogates. In order to validate these models, we developed a dedicated EMA test bench (Figure 1) intended to replicate the operating condition experienced by common flight control actuators. The bench is highly modular, allowing to easily replace components and test different EMA architectures. In order to contain costs and time associated to the development, we made extensive use of off-the-shelf hardware; most of the custom designed parts were manufactured through rapid prototyping techniques.
The test bench is able to simulate the operation of the actuator in nominal conditions and in presence of incipient mechanical faults, namely a variation of friction and an increase of backlash in the reduction gearbox. Sensitivity to electrical fault modes will be included in a future upgrade. The output of the test bench was compared to the predictions of numerical models in nominal conditions. The results showed a good matching between the two systems, which is promising for the use of such models within real-time health monitoring routines.

*Keywords*: Experimental validation, Lumped parameter models, Test bench, Electromechanical Actuator (EMA).

## 1. Introduction

Most approaches to Prognostics and Health Management (PHM) rely either on model-based or data-driven methodologies, or on a combination of the two. In common strategies for Model-based PHM, a physics-based digital twin of the system is employed to monitor the behaviour of its physical counterpart: the response of the monitored equipment is compared to that of the model, and the discrepancies are analysed in search of early signs of incipient faults. By contrast, data-driven methodologies rely on machine learning algorithms, trained offline to identify failures from the measured response of the monitored system.

In either case, physics-based models of the monitored system are required in the process. In model-based approaches they are employed directly in the PHM process, while in data-driven approaches they are employed to generate the datasets needed to train the machine learning algorithms: indeed, field data is usually insufficient to characterize efficiently the behaviour of a system in presence of unlikely events like failures.

Ekanayake et al. (2019) provides a review of model-based strategies for fault detection and failure prognosis. Gorinevsky et al. (2002) employ detailed physical models to detect incipient faults of aircraft Auxiliary Power Units (APUs). Cubillo et al. (2016) compare several model-based approaches available in literature applying them to mechanical equipment such as gears and bearings. A review of data-driven approaches to PHM is proposed by Soualhi et al. (2019). Tobon-Mejia et al. (2012) propose a combination of Wavelet Packet Decomposition (WPD) and Gaussian Hidden Markov Models to predict failures of rotating equipment. A regression model based on Multi-Layer Perceptrons (MLPs) is employed for failure prognosis of aircraft turbine engines by Elattar et al. (2018). Representative physics-based models of an engineering system shall reproduce the operation of the monitored equipment with high accuracy in a wide variety of operational scenarios. In addition, for PHM applications the computational time is often a critical feature: for model-based PHM the models are usually required to run in real-time, while the training datasets for machine learning approaches must include a high number of simulation. Hence, physics based models shall combine accuracy and representativeness with a suitable computational time.

*Proceedings of the 31st European Safety and Reliability Conference*
*Edited by* Bruno Castanier, Marko Cepin, David Bigaud, and Christophe Berenguer
*Published by* Research Publishing, Singapore.
ISBN: 978-981-18-2016-8; doi:10.3850/978-981-18-2016-8_560-cd

For this reason, lumped parameter dynamical models are preferred to finite elements simulations where possible (Dalla Vedova et al., 2019).

In order to guarantee that the models reflect the behaviour of the monitored system, a validation campaign shall be carried out, either leveraging field data acquired during the operation of the equipment, or collecting experimental measurements on a physical test bench that simulates the real operating conditions of the system.

In this work, we describe the development of a dedicated test bench for the validation of PHM models of Electromechanical Actuators (EMAs) for aircraft flight controls. These devices use an electric motor and a transmission to control the position of a mechanical element. In aerospace and other vehicle applications, they are gradually replacing more traditional actuation technologies based on hydraulic and pneumatic power, providing better performances in terms of efficiency, weight and fuel consumption (Howse, 2003 and Garcia Garriga et al, 2018). Our test bench includes an industrial servomotor controlled in closed loop. It is connected to a custom mechanical transmission and a load simulator that reproduces the aerodynamic forces acting on a flight control actuator. A preliminary validation of the actuator models consisted in the comparison of its response with that of the test bench, and showed a promising matching between the two.

In this paper, Section 2 describes the lumped parameter dynamical model to be validated. Section 3 provides an overview of the test bench architecture. Section 4 discusses the results of the comparison between the model and the physical test bench.

## 2. Electromechanical Actuator Model

This work presents the experimental validation of a high fidelity, lumped parameter model of an electromechanical actuator. The model was initially presented and discussed in detail by Berri et al. (2018a) for actuator architectures based on Brushless DC (BLDC) motors, and subsequently extended to Permanent Magnet Synchronous Motors (PMSM) (Berri et al, 2018b). The model is highly modular, and lends itself to be employed as a representation of different EMA layouts, characterized by different motors, mechanical transmissions, or control laws.

The model includes five main blocks that mirror the major subsystems of a physical EMA, namely:

- *Control electronics*: this block accepts in input the actual state of the actuator, in terms of position and speed, and the corresponding setpoints. The output of the block is the torque/current setpoint requested to the motor
- *Motor power electronics*: this block manages the current/torque closed loop control of the brushless motor, as well as the phase commutation to keep the magnetic field of the stator synchronized with the angular position of the rotor and generate the requested torque. It accepts in input the measured phase currents flowing in the motor coils, as well as the current setpoint and the rotor angular position; the output of the block are the voltages applied to each phase of the motor. To speed up computations, the current control loop has a simplified architecture compared to that of the test bench; this may result in some discrepancies in the direct current and voltage signals.
- *Motor electromagnetic model*: this block includes the three-phase equivalent RL circuit of the stator to compute the current flowing in the motor coils. In addition, the magnetic coupling of the rotor and stator is solved to determine the instantaneous torque generated by the motor.
- *Motor-transmission mechanical model*: this block simulates the response of the mechanical branch of the EMA with a second order dynamical model. Several nonlinear effects are taken into account in the simulation, including: mechanical endstops, dry friction, and backlash.
- *Load simulator*: this block simulates the external load on the actuator. In previous works, it employed the aerodynamic model of the F-16 fighter jet available from Stevens et al. (2015), here replaced by a model of the physical load simulator installed on the test bench.

A schematic representation of the model is given by the block diagram of Figure 1, highlighting the information flow between the different subsystems.

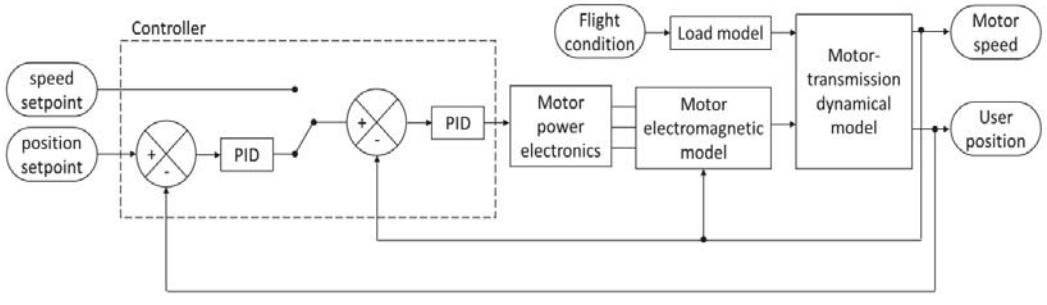


Figure 1: Block diagram of the EMA dynamical model

## 3. EMA test bench

A dedicated test bench was developed with the purpose of validating the response of the model described in Section 2 by the comparison with physical data. The test bench features a modular architecture that mirrors that of a typical electromechanical actuator for flight controls. The following sections describe in detail the major components and subsystems of the actuator.

### 3.1. *Motor-Driver*

The actuation section of the test bench employs off the shelf hardware designed for industrial automation applications. This choice allowed to reduce costs and time associated with the design and development of the test bench, while keeping a high representativeness of the aerospace components considered in the study. Indeed, despite the higher cost and lower weight, aerospace EMAs share the same basic architecture and operating principles of industrial ones. Specifically, a Siemens 1FK7060-2AC71-1QA0 permanent magnet, three-phase, 8-poles synchronous motor is driven by a three-phase inverter at 400V. The motor has a rated power of 1.1 kW at 2000 rpm, with a torque coefficient of 1.91 Nm/A.

Its main characteristics are summarized in Table 1.

The inverter controls the phase commutation and acts as a data logger for the electrical parameters of the motor, allowing to measure currents, voltages and rotor position and speed with a sampling frequency of 400 Hz.

### 3.2. *Transmission*

Aerospace electromechanical actuators often use a high gear ratio mechanical transmission to connect the motor to the external load. This gearbox must be compact, lightweight, and highly efficient. For the test bench we developed a particular layout of a Wolfrom drive (Lopez Garcia et al., 2019), able to combine all these characteristics. The transmission is a custom design achieving a 124:1 gear ratio with a very compact form factor and low inertia (Berri et al., 2020), making wide use of Fused Filament Forming (FFF) additive manufacturing for a rapid and low cost prototyping. The mechanical efficiency was measured at 65%, a high value considering the poor tolerances of FFF gears, and allows is to be back-driven with a reverse efficiency of 51%.

The output of the gearbox is connected to a high resolution, 5000 pulses per revolution, incremental encoder that allows to close the position control loop

Table 1. Datasheet of the test bench motor.

| Model | | 1FK7060 |
|---|---|---|
| Number of poles | (-) | 8 |
| Torque coefficient | (Nm/A) | 1.91 |
| Phase resistance | (Ω) | 2.75 |
| Phase inductance | (mH) | 30.5 |
| Max voltage | (V) | 400 |
| Peak current | (A) | 10.7 |
| Max speed | (rpm) | 7200 |
| Peak torque | (Nm) | 18 |
| Rotor inertia | (kg $m^2$) | 0.00077 |
| Mass | (kg) | 7.1 |

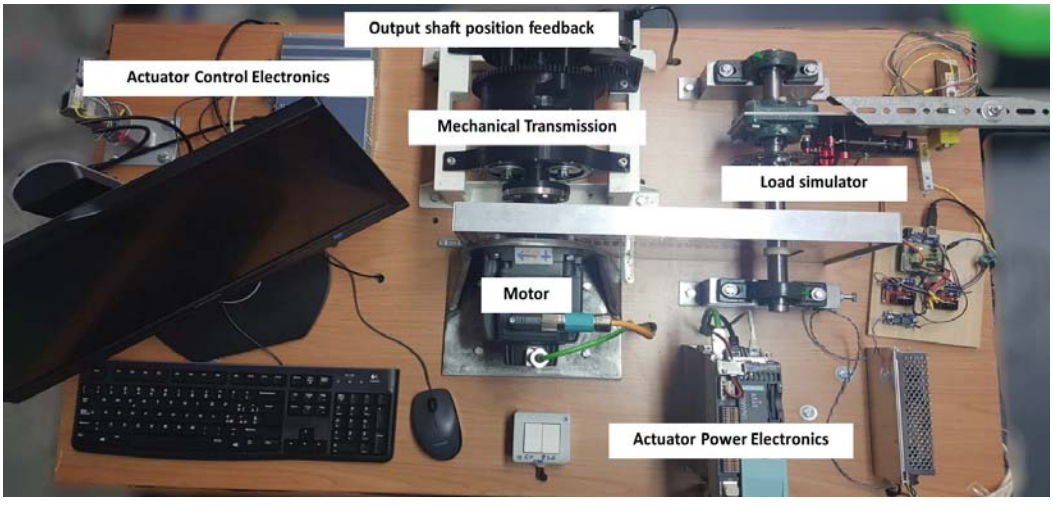


Figure 2: Picture of the EMA test bench

### 3.3. *Load simulator*

To simulate the aerodynamic load on the actuator we employed a disc brake connected able to apply a torque controlled in closed loop. Specifically, the brake calliper assembly is installed on a pair of bearings on the shaft that carries the brake disc. A load cell bounds the rotation of the calliper assembly about the axis of the shaft: as a result, the force measured by the load cell is proportional to the braking torque. As the main transmission of the test bench is not able to transmit the maximum torque of the motor, a secondary, roller-chain transmission connects the motor shaft directly to the brake disc. The gear ratio in this case is limited to 1.48:1, and allows to employ a relatively small brake to simulate a significant load on the motor. A small, hobby-grade servo actuates the brake calliper, driven by a microcontroller that reads the loadcell and allow to apply a repeatable braking torque through a Proportional-Integrative (PI) control loop

## 4. Results

To validate the response of the EMA model we compared its behavior to that of the physical test bench. We tested step setpoints in speed and position, with and without an external load. The comparison was done in terms of user position and speed, and motor voltage and current for a given command.

### 4.1. *Speed Control Mode*

In speed control mode, the actual position of the system is not fed back to the controller. A step setpoint of 300rpm amplitude is compared to the motor speed to compute a current/torque setpoint fed to the motor driver. Figures 3 to 6 compare different key signals measured on the test bench and dynamical model.

Figure 3 shows the speed setpoint (blue curves) and actual speed (red curves) of the motor for the two systems. The response of the test bench is represented with a continuous line, while that of the model is a darker, dashed line. The actuator reaches the speed setpoint in about ten milliseconds, after an overshoot and some damped oscillation.

Figure 4 shows the current component of the PMSM in the quadrature direction, i.e. 90° in advance of the rotor orientation. This current is proportional to the produced torque and is obtained from the phase currents with the Clarke-Park transformations (O'Rourke et al., 2019). The current along the direct axis (i.e. aligned with the rotor) is shown in Figure 5; as this component does not generate any torque, it is usually commanded to zero.

The voltage applied to the motor coils in the quadrature direction is represented in Figure 6: as this test is performed in a no-load condition, the voltage is approximately proportional to motor speed and equal to the back-EMF of the motor.

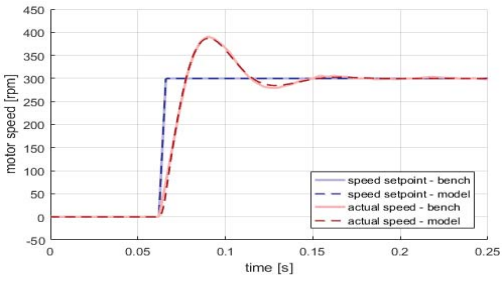


Figure 3: Commanded and actual speed in speed control mode.

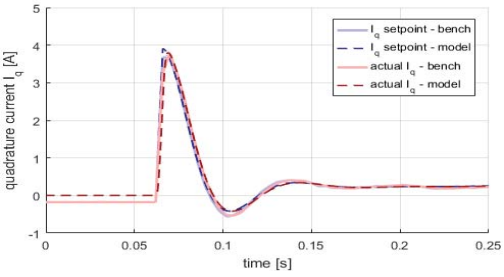


Figure 4: Commanded and actual quadrature current in speed control mode.

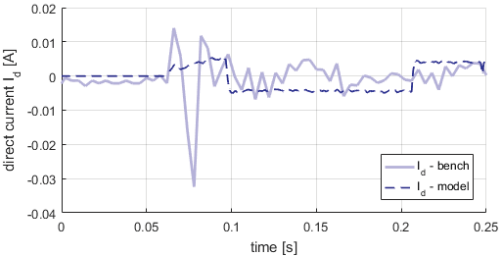


Figure 5: Direct current in speed control mode.

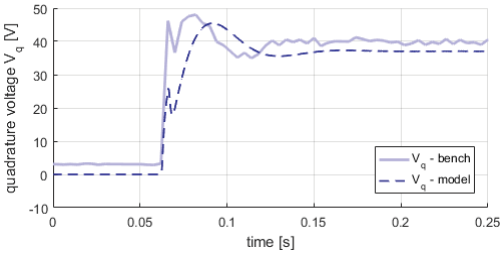


Figure 6: Quadrature voltage in speed control mode.

The dynamical model is generally able to predict the behaviour of the physical test bench with satisfying accuracy. The speed and quadrature current signals are reproduced with a very small error; a higher discrepancy can be found in the voltage signal, as a result of the simplified current control strategy that replaces the adaptive PI controller of the physical system with a computationally cheaper hysteresis control loop.

### 4.2. *Position Control Mode*

In position control mode, the setpoint of the actuator is compared to the output speed to compute a speed setpoint through a PID controller. The rest of the control logic works as in the previous case. The specific setpoint signal given to the system is a 60° step on the user axis; the software limitations on maximum speed and acceleration result in the blue curve of Figure 7 as the actual setpoint seen by the controller.

Figure 8 shows that the commanded motor speed is matched accurately both by the system and its model. The overshoot that was visible in Figure 3 is mitigated by the more gradual command.

A small braking torque was produced by the load simulator; as a result, the current has the behaviour shown by Figure 9, where the high frequency ripple reflects the torque ripple produced by a small misalignment of the brake disc. This ripple is slightly undersampled by the brake loadcell of the test bench: then, the model predicts a smaller current ripple amplitude.

Figure 10 and 11 report the direct current and quadrature voltage signals, respectively. Similarly to the previous tests, the model replicates with moderate accuracy the motor voltage, while the direct current is captured with a large error, in particular when the motor speed is high. This behaviour is motivated by the different architectures of the current controllers of the model and test bench: at high speed, the adaptive control law of the test bench differs from the simulation, that is calibrated at low speeds.

## 5. Conclusions

A dedicated test bench was developed to validate the accuracy of lumped parameter models of electromechanical flight control actuators. The test bench allows to reproduce the behaviour of an aircraft flight control actuator and to simulate different operational scenarios for the system. It features a modular architecture to ease future upgrades, such as the installation of additional sensors A high fidelity dynamical model of flight control EMAs was compared to the test bench in terms of step response in speed and position control modes. The prediction of the model agrees with the measurements from the test bench with promising accuracy, which is promising for employing the models to collect databases for training of data-driven PHM strategies.

Future developments will include the characterization of the system behaviour in a wider range of conditions, including the simulation of incipient faults of the electrical and mechanical subsystems of the actuator, to validate the model in these conditions, as well as to assess the performance of different PHM methodologies.

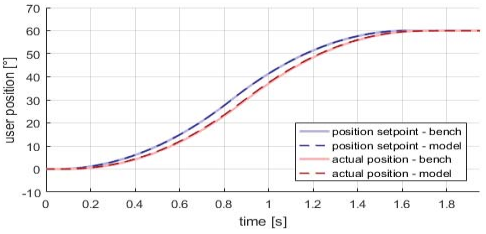


Figure 7: Commanded and actual position in position control mode.

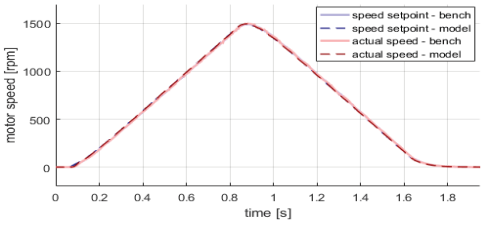


Figure 8: Commanded and actual speed in position control mode.

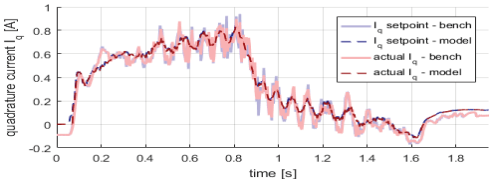


Figure 9: Commanded and actual quadrature current in position control mode.

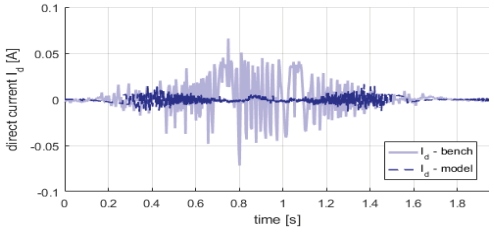


Figure 10: Direct current in position control mode.

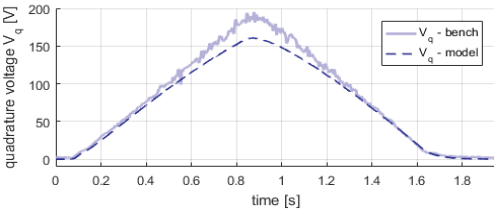


Figure 11: Quadrature voltage in position control mode.

**Acknowledgement**

The authors wish to thank the Master's thesis students Pietro Sciandra and Valentina Boschetti for their invaluable support in the development of the test bench. A special acknowledgement to Scuola Camerana (https://www.scuolacamerana.it) for their support in manufacturing some of the mechanical components of the test bench.

**References**

Berri, P.C., Dalla Vedova, M.D.L. and Maggiore, P. (2018a). A Lumped Parameter High Fidelity EMA Model for Model-Based Prognostics. *29th European Safety and Reliability Conference (ESREL 2018)*, Hannover, Germany.

Berri P.C., Dalla Vedova, M.D.L., Maggiore, P. and Scanavino, M. (2018b). Permanent Magnet Synchronous Motor (PMSM) for Aerospace Servomechanisms: Proposal of a Lumped Model for Prognostics. *2nd European Conference on Electrical Engineering & Computer Science (EECS 2018)*. Bern, Switzerland.

Berri, P.C., Dalla Vedova, M.D.L., Maggiore, P. and Riva, G. (2020). Design and Development of a Planetary Gearbox for Electromechanical Actuator Test Bench through Additive Manufacturing. *Actuators Vol. 9, no. 2,* 35.

Cubillo, A., Perinpanayagam, S. and Esperon-Miguez, E. (2016). A review of physics-based models in prognostics: Application to gears and bearings of rotating machinery. *Advances in Mechanical Engineering Vol. 8 no. 8*, 1–21.

Dalla Vedova, M.D.L., Berri, P.C., Corsi, C. and Alimhillaj, P. (2019). New synthetic fluid dynamic model for aerospace four-ways servovalve. *International Journal of Mechanics and Control Vol. 20 no. 2*, 105-112.

Ekanayake, T., Dewasurendra, D., Abeyratne, S., Ma, L. and Yarlagadda, P. (2019). Model-based fault diagnosis and prognosis of dynamic systems: a review, *Procedia Manufacturing, Vol. 30*, 435-442.

Elattar, H.M., Elminir, H.K. and Riad, A.M. (2018). Towards online data-driven prognostics system. *Complex Intell. Syst. Vol. 4*, 271–282.

Garcia Garriga, A., Ponnusamy, S.S. and Mainini, L. (2018). A multi-fidelity framework to support the design of More-Electric Actuation. *2018 Multidisciplinary Analysis and Optimization Conference* (AIAA 2018-3741).

Gorinevsky, D., Nwadiogbu E. and Mylaraswamy, D. (2002). Model-based diagnostics for small-scale turbomachines. *Proceedings of the 41st IEEE Conference on Decision and Control*, Las Vegas, NV, USA, vol.4, pp. 4784-4789.

Howse M. (2003). All electric aircraft. *IEEE Power Engineering Journal, Vol. 17 no. 4*, 35–37.

Lopez Garcia, P., Crispel, S., Verstraten, T., Saerens, E., Vanderborght, B. and Lefeber, D. (2019). Wolfrom Gearboxes for Lightweight, Human-Centered Robotics. *International Conference on Gears*. Munich, Germany.

O'Rourke, C.J., Qasim, M.M., Overlin, M.R. and Kirtley Jr, J.L. (2019). A Geometric Interpretation of Reference Frames and Transformations: dq0, Clarke, and Park. *IEEE Transactions on Energy Conversion, Vol. 34, no. 4*, 2070-2083.

Soualhi, A., Razik, H. and Guy, C. (2019). Data Driven Methods for the Prediction of Failures. *IEEE International Symposium on Diagnostics for Electric Machines, Power Electronics and Drives (SDEMPED 2019)*, Tolouse, France.

Stevens, B.L., Lewis, F.L., Johnson E.N. (2015). *Aircraft Control and Simulation: Dynamics, Controls Design, and Autonomous Systems*, 3rd Edition, Wiley-Blackwell.

Tobon-Mejia, D., Medjaher, K., Zerhouni, N. and Tripot, G. (2012). A data-driven failure prognostics method based on mixture of gaussians hidden markov models. *IEEE Transactions on Reliability, Institute of Electrical and Electronics Engineers, Vol. 61 no. 2*.